Ab Initio Study of the Reactions of OH Radical with 2,5-Dimethylfuran

T. Ferraz-Santos, G. F. Bauerfeldt*
Departamento de Química, Instituto de Ciências Exatas, Universidade Federal Rural do Rio de Janeiro, RJ, Brazil

Abstract
In this work, the potential energy surface for the 2,5-dimethylfuran + OH reaction is detailed described at the Density Functional Theory level and rate coefficients are calculated on the basis of the variational transition state theory. Both OH addition and H abstraction channels are considered. For the addition paths, our results indicate that the formation of a pre-reaction complex is determinant only for temperatures below 550 K. In agreement with the literature, rate coefficients indicates that OH addition paths are important under low temperature conditions, while H abstraction channels are only achieved at typical combustion temperatures.

1. Introduction

Biofuels, which can be obtained from renewable and abundant resources, have been the subject of numerous publications. Several molecules can be produced from biomass, however furan derivatives have received special attention [1-3].Among these, 2,5-dimethylfuran (DMF) is a promising substitute for gasoline in a future scenario.

Recent studies indicate several advantages of using DMF over ethanol, the most abundantly biofuel consumed worldwide, including higher energy density, higher boiling point and lower solubility in water [3,4].

Since the report of these promising production methods [5-9], experimental and theoretical studies on combustion and pyrolysis of DMF have ensued. Sirjean and co-workers[10] proposed a detailed kinetic model for the oxidation of DMF. Their results were in good agreement with shock tube ignition delay time measurements and the pyrolysis study performed by Lifshitz et al. [11]. The abstraction by OH radicals was considered a crucial reaction in both pyrolysis and oxidation simulations, in which the rate coefficients were taken from the *ab initio* study of Simmie and Metcalfe [2]. Since no kinetic data at high temperatures had been previously reported for the OH-addition reaction, the rate coefficients were considered analogous to the furan + OH reaction and the corresponding values were taken from the work of Atkinson and Arey [12], even though these rate coefficients had been reported at temperatures lower than the temperature range in that DMF oxidation simulation study [10].

Reactions of DMF with the OH radical are also expected in a post-combustion scenario, since furans can be directly emitted into the atmosphere from burning fossil fuels and can also be formed in situ from isoprene [13-15]. The addition path is preferable under atmospheric conditions as shown by Zhang and colleagues [16], in their theoretical work for 3-methlyfuran + OH reaction. The room temperature rate coefficient for the DMF + OH reaction has been reported by Bierbach and co-workers as (13.21 ± 0.92)x10^{-11} cm^3 $molec^{-1}$ s^{-1} [17].

In this work, our main goal is to describe in details the potential energy surface of the reactions of DMF + OH, including theoretical calculations of rate coefficients, using the canonical and microcanonicalvariational transition state theory.

2. Calculation methods

The optimized geometries and frequencies of the reactants, products, pre-barrier complexes and saddle points were calculated at the Density Functional Theory (DFT) level [18-19] using the BHandHLYP functional along with the aug-cc-pVDZ basis set [20].The characterization of the stationary points as a local minima or transition states were performed by the analysis of the vibrational frequencies. The intrinsic reaction coordinate (IRC) method[21] was used to calculate the minimum energy path connecting the reactants or the pre-barrier complex to the products, passing through the saddle point. On the other hand, scan calculations were carried out for the description of the reaction path connecting the pre-barrier complex and reactants. All the theoretical calculations were performed using the Gaussian03 suite of programs [22].

Using conventional statistical thermodynamics relations, the vibrationally adiabatic potential energy curve was transformed into a Gibbs free energy curve at each temperature. The function *G(s,T)*, being *s* the reaction coordinate, was analytically maximized to obtain the *s* value that corresponds to the location of the transition state and its properties were applied as the input for the conventional Eyring equation [17], obtaining canonical variational transition state theory (CVTST) rate coefficients over the temperature range200-1000 K. For the unimolecular reactions, microcanonical variational transition state theory (mCVTST) rate coefficients were also calculated, according to the methodology described elsewhere [23].

3. Results and discussion

The optimized structures of all stationary points are shown in Figure 1.The relative energies for all species involved in both addition and abstraction paths of the OH + 2,5-dimethylfuran are presented in Table 1. To better understand the reaction mechanisms, these two pathways will be discussed separately.

* Corresponding author: bauerfeldt@ufrrj.br

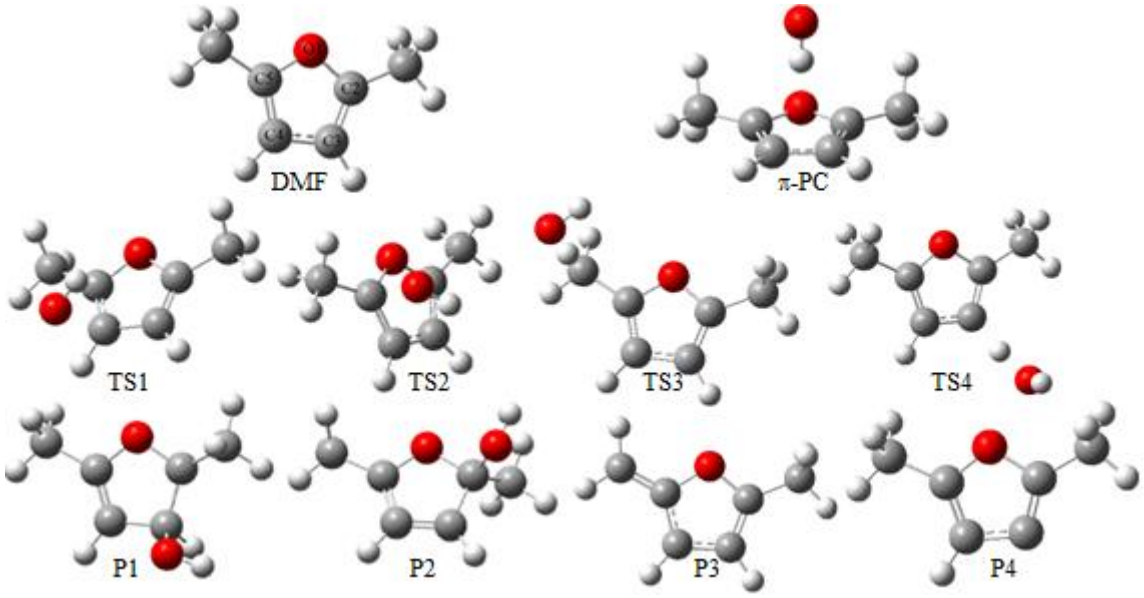

Fig. 1. The structures for reactants, pre-barrier complex, saddle points and products along the DMF + OH reaction profile.

Table 1
Relative energies (in kcal mol^{-1}) for the stationary points along the DMF + OH reaction path, in relation to the isolated reactants.

	ΔE [a]	**ΔE^0** [b]
Reactants - DMF + OH	0,00	0,00
PC-π	-3.73	-2.78
TS1	0.51	2.22
TS2	-2.98	-1.37
TS3	3.38	1.80
TS4	14.05	11.92
P1	-16.27	-12.73
P2	-33.64	-30.40
P3+H_2O	-28.65	-29.04
P4+H_2O	6.21	6.52

[a] : Relative energies at 0 K
[b] : Relative energies at 0 K, corrected by the zero-point vibrational energies.

3.1. Addition channels

There are two possible OH addition reactions to the π system in the molecule of DMF, *i.e*, the addition at C3 (or C4) or the addition at C2 (or C5), via the saddle points denoted as TS1 and TS2, respectively, which are directly connected to the products P1 and P2. As mentioned before, no other theoretical results are available in the literature for the addition reaction between the OH radical and DMF, so we compare our results with additional results available in the literature for other methylfurans, when such comparisons are possible and reasonable.

Our results are in agreement with the strong belief founded in the literature that the OH addition to unsaturated molecules occurs via a pre-barrier complex, an intermediate stabilized in relation to the reactants by a few kcal mol^{-1}. The geometry of such intermediate (Figure 1) shows the hydrogen of the OH radical perpendicularly pointing to the plane that contains the double bonds, charactering the pre-barrier complex as π–type (π–PC). Comparing the geometries of the isolated reactant and the π–PC, no considerable changes are observed for the C2-C3 (or C5-C4) and the C3-C4 bond distances, which are 1.351 Å and 1.436 Å for DMF and 1.354 Å and 1.438 Å for π–PC, respectively. The π–PC is stabilized in relation to the isolated reactants by 3.73 kcal mol^{-1} and including zero-point correction the stabilization is set at 2.78 kcal mol^{-1}. Since the structural change in the ring of DMF is irrelevant, we assumed that the stabilization of the π–PC can be explained by thermodynamics aspects. The path that connects the π–PC and initial reagents is barrierless which makes an IRC analysis unfeasible, so the reaction path was obtained using scan calculations. The distance, in angstroms, of the oxygen atom of the OH radical to an imaginary point located between the C3-C4 interatomic distance was used as the scan coordinate.

As expected, both saddle points TS1 and TS2 are located above the π–PC. However, with respect to the isolated reactants, TS1 is placed above them notwithstanding TS2 is below, as shown in Table 1. These observations suggest that addition to C2 is energetically favored in regard to the C3 addition.

The IRC procedure calculates minimum energy paths starting from the optimized geometries of the saddle points. The products of the C3 and C2 additions, generally known as OH-adducts, P1 and P2, respectively, are located at the end of these reactions paths. However, at the reactants region of the IRC, a

common intermediate is reached at both calculations, which structure corresponds to the π–PC. Therefore, the mechanism for both addition reactions can be described by a reversible pre-barrier complex formation reaction, followed by the irreversible formation of either P1 or P2 adducts. An analysis of the vibrational frequencies confirms that the structures of P1 and P2 correspond to stationary points in the PES. The adducts are considerably stabilized in relation to the isolated reactants, which relative energies are -16.27 kcal mol^{-1} and -33.64 kcal mol^{-1}, for P1 and P2, respectively. Zhang and co-workers [24] in their work with the reaction of OH and 2-methylfuran (2MF) using G3MP2B3/6-31G(d,p)//B3LYP /6-311G(d,p) calculations located 4 adducts for OH addition at C2, C3, C4 and C5, and the addition at C2 and C3 for 2MF and DMF are somehow related. The relative energies of Zhang's adducts in relation to the isolated reactants are -16.42 kcal mol^{-1} and -31.67 kcal mol^{-1} for C3 and C2 addition, respectively, which are very similar to the relative energies of P1 and P2 adducts of DMF. No saddle points or pre- reaction complex for addition reactions were reported in their study, therefore no further comparisons are possible.

3.2. Abstraction channels

The abstraction of H atom by OH can occur through two distinct pathways: H-abstraction from the CH_3-group and H-abstraction from the hydrogen atoms in the furan ring. Two stable saddle points were located for these channels, denoted as TS3 and TS4, for abstraction at the CH_3-group and at the furan ring, respectively, which directly correlates to products P3+H_2O and P4+H_2O.

The analysis of the potential energy surface for both abstraction pathways reveals that these reactions proceeds via direct channels from reactants to products, without formation of a pre- or post-reaction complex.

Barrier heights suggest that abstraction at the methyl site are more feasible that at the furan ring, as shown by relative energies for TS3 and TS4 in Table 1. The energy barrier for abstraction from the methyl group obtained with BHandHLYP/aug-cc-pVDZ is ~2 kcal mol^{-1} lower than that reported by Simmie and Metcalfe [1] in their study of the same reaction using G3 compound method, even though the G3 barrier for abstraction from the furan ring is lower than our DFT value by about 3 kcal mol^{-1}. Although the results may seem conflicting, it is important to highlight that even at elevated temperatures abstraction from the ring must have limited significance, since a previous work [25] has shown from theoretical calculations that the ring C-H bond is extremely strong, estimated at 120 kcal mol^{-1}.

3.3. Validation of the electronic energies

In order to guarantee the quality of our DFT data, attempts to validate our BHandHLYP/aug-cc-pVDZ were performed. Since most of the stationary points (DMF, π-PC, saddle points and products – excluding H_2O) are bulky molecules, the use of high accurate *ab initio* methods is unfeasible. So, single point calculations at QCISD(T)/aug-cc-pVDZ and CCSD(T)/aug-cc-pVDZ were performed on the basis of the BHandHLYP/aug-cc-pVDZ optimized geometries. Although QCISD(T)/aug-cc-pVDZ//BHandHLYP/aug-cc-pVDZ single point energy calculations presented convergence problems for TS4, CCSD(T)/aug-cc-pVDZ//BHandHLYP/aug-cc-pVDZ results seem very promising. They confirm the reaction profiles and diminish the barrier heights for reactions 1, 3 and 4, which are linked to TS1, TS3 and TS4, respectively. However, the structure of TS2 is stabilized in respect to the π-PC, suggesting a barrierless direct mechanism from reactants to products. This mechanism is not supported by previous literature results for alkylfurans, and it is clear that when using single point corrections even small differences at the optimized geometries may propagate significant errors, modifying the reaction profile. So, these QCISD(T)/aug-cc-pVDZ//BHandHLYP/aug-cc-pVDZ and CCSD(T)/aug-cc-pVDZ//BHandHLYP/aug-cc-pVDZ results could not be considered to rate coefficients calculations at this point of our work.

3.4. Canonical rate coefficients

Addition reactions. Canonical rate coefficients were calculated for the formation and dissociation reactions of the π–PC and subsequent addition of OH radical to the π–PC, represented by the model:

$$\text{.DMF} + \text{OH} \rightarrow \text{PC-}\pi,\ k_1$$

$$\text{PC-}\pi \rightarrow \text{DMF} + \text{OH},\ k_{-1}$$

$$\text{PC-}\pi \rightarrow \text{P1},\ k_2^1$$

$$\text{PC-}\pi \rightarrow \text{P2},\ k_2^2$$

Molecular properties obtained at BHandHLYP functional with aug-cc-pVDZ basis set were used to calculate canonical variational transition state theory rate coefficients. Adopting the steady-state approximation, a global rate coefficient for addition reactions could be calculated as shown by the following expression (since the molecule of DMF is symmetric, the factor 2 accounts for the degeneracy of the reaction path):

$$k_{add} = 2 \times \left(\frac{k_1 k_2^1 + k_1 k_2^2}{k_{-1} + k_2^1 + k_2^2}\right) \quad (1)$$

.The k_{-1} rate coefficients were calculated using molecular properties of 40 points along the potentialcurve representing the dissociation of the π–PC into the isolated reactants, DMF and OH. A very similar tendency was observed for the enthalpy, entropy and vibrationally adiabatic potential profiles, which increased along with the reaction coordinate. At lower temperatures, the enthalpy and entropy curves are located above those calculated at higher temperatures. At any temperature, the entropy curve has a substantial increasing profile, since the reaction path evolves from

a tighter to a looser structure. In order to evaluate the k_1 rate coefficient, the microscopic reversibility was assumed. The calculated k_1 and k_{-1}rate coefficients are shown in Table 2.

In the variational procedure adopted for the calculation of $k_2^1$and k_2^2 rate coefficients, molecular properties of 21 points along the reaction coordinate were used. The vibrationally adiabatic potential curve shows a maximum value slightly displaced from $s = 0$ to positive values. This fact can be explained by the increase of the vibrational frequencies observed when the reaction path progresses from a reactant-like structure to a product-like structure. However, the enthalpy curves reveal maximum values located at $s = 0$ for all the temperature range of this study. The entropy is a decreasing function of reaction coordinate and maximum values of the Gibbs free energy function, $\Delta G(s,T)$, are located at positive reaction coordinate values increasing with the temperature. As expected by the energies barriers, the k_2^1 rate coefficients are substantially higher than the k_2^2coefficients, implying that the formation of P1 is favored by both thermodynamics and kinetics aspects. The calculated k_2^1 and k_2^2 rate coefficients are also shown in Table 2.

The proposed model was satisfactory to represent the reaction path at temperatures below 500 K, showing the global rate coefficient k_{add} as a decreasing function of the temperature. However, at temperatures above 550 K we noticed a change in the mechanism. Therefore, in the temperature range of 550-1000 K, the evaluation of k_{add} took into account new$k_1'$and k_2' values, which corresponds to the rate coefficients for the reaction of DMF + OH directly leading to the formation of P1 and P2, respectively, as follows:

$$k_{add} = 2 \times (k_1' + k_2') \quad (2)$$

These results suggest that the formation of the pre-barrier complex, π–PC, becomes less important in the global mechanism with the increase in temperature. At higher temperatures, the reaction path would develop via a direct channel from the reactants to the product, overcoming an energy barrier represented by the energy of the saddle point.

Abstraction reactions. Since the abstraction reactions proceeds without the formation of a pre or post-reaction complexes, the representative mechanism is simple, as shown below:

$$DMF + OH \rightarrow P3 + H_2O, k_3$$
$$DMF + OH \rightarrow P4 + H_2O, k_4$$

The global rate coefficient for abstraction reactions, k_{abs}, could be calculated as shown by the following expression (since the molecule of DMF is symmetric, the factor 2 accounts for the degeneracy of the reaction path):

$$k_{abs} = 2 \times (k_3 + k_4) \quad (3)$$

The k_3 and k_4 rate coefficients were calculated using the same procedure adopted for evaluation of $k_1'$and k_2'.Due the high energy barrier for abstraction at methyl site, represented by k_3, it is safe to say that H abstraction by OH radical is likely to occur exclusively at the alkyl side chain. The k_3, k_4 and the k_{abs} rate coefficients are shown in Table 3.

3.5. RRKM calculations

For the calculation of the addition rate coefficients, in the range of temperatures up to 500 K, the assumption that the equilibrium is reached at the canonical level for the first step of the mechanism, DMF + OH = π-PC, may be a source of error on thecanonical variational procedure if the π-PC is not thermalized.

Table 2
The canonical variational rate coefficients for addition reactions: k_1(cm³ molec^{-1} s^{-1}),k_{-1},k_2^1 and k_2^2(s^{-1}) andk_1', k_2' and k_{add}(cm³ molec^{-1} s^{-1}) calculated at the BHandHLYP/aug-cc-pVDZ level at different temperatures.

Temperature (K)	k_1 (cm³molec^{-1}s^{-1})	k_{-1} (s^{-1})	k_2^1 (s^{-1})	k_2^2 (s^{-1})	k_1' (cm³molec^{-1}s^{-1})	k_2' (cm³molec^{-1}s^{-1})	k_{add} (cm³molec^{-1}s^{-1})
200	1.73x10^{-10}	2.73x10^{11}	7.00x10^{5}	3.39x10^{9}	-	-	4.24x10^{-12}
300	1.05x10^{-10}	1.28x10^{12}	3.69x10^{7}	8.18x10^{9}	-	-	1.34x10^{-12}
400	7.97x10^{-11}	2.26x10^{12}	2.55x10^{8}	1.21x10^{10}	-	-	8.68x10^{-13}
500	6.83x10^{-11}	2.88x10^{12}	7.93x10^{8}	1.51x10^{10}	-	-	7.50x10^{-13}
550	-	-	-	-	2.53x10^{-14}	3.45x10^{-13}	7.40x10^{-13}
600	-	-	-	-	3.29x10^{-14}	3.40x10^{-13}	7.46x10^{-13}
700	-	-	-	-	5.14x10^{-14}	3.45x10^{-13}	7.93x10^{-13}
800	-	-	-	-	7.46x10^{-14}	3.63x10^{-13}	8.75x10^{-13}
900	-	-	-	-	1.03x10^{-13}	3.90x10^{-13}	9.85x10^{-13}
1000	-	-	-	-	1.36x10^{-13}	4.23x10^{-13}	1.12x10^{-12}

Table 3
The canonical variational rate coefficients for addition reactions: k_3, $k_4$and k_{abs}(cm³ molec^{-1} s^{-1}) calculated at the BHandHLYP/aug-cc-pVDZ level at different temperatures.

Temperature (K)	k_3 (cm³ molec^{-1} s^{-1})	k_4 (cm³ molec^{-1} s^{-1})	k_{abs} (cm³ molec^{-1} s^{-1})
200	3.34 x 10^{-15}	6.38 x 10^{-26}	6.67 x 10^{-15}
300	3.30 x 10^{-14}	1.43 x 10^{-21}	6.60 x 10^{-14}
400	1.05 x 10^{-13}	2.61 x 10^{-19}	2.10 x 10^{-13}
500	2.17 x 10^{-13}	6.75 x 10^{-18}	4.34 x 10^{-13}
600	3.64 x 10^{-13}	6.46 x 10^{-17}	7.28 x 10^{-13}
700	5.45 x 10^{-13}	3.10 x 10^{-16}	1.09 x 10^{-12}
800	7.59 x 10^{-13}	1.10 x 10^{-15}	1.52 x 10^{-12}
900	1.01 x 10^{-12}	3.06 x 10^{-15}	2.02 x 10^{-12}
1000	1.29 x 10^{-12}	7.14 x 10^{-15}	2.60 x 10^{-12}

The thermal equilibrium could only be achieved in the canonical partition after the intermediate has been trapped for enough time at the potential well, before the following reaction steps occur. A final validation of the CVT rate coefficients must be then assessed by the calculation of the same rate coefficients at the mCVT.

In a two-transition state model proposed by Greenwald and co-workers [26], although the canonical equilibrium is not reached, restrictions of energy and angular momentum must be respected, and then a microcanonical partition is achieved. For each *E* and *J*, an outer and an inner transition state are located, $N_1$and N_2, and both are used to calculate an effective sum of states, N_{eff}:

$$\frac{1}{N_{eff}} = \frac{1}{N_1} + \frac{1}{N_2} \quad (4)$$

Since the two reactions of the π-PC to form the addition adducts cannot be considered separately, a minor adjustment in Greenwald's expression for the effective sum of states is proposed:

$$\frac{1}{N_{eff}} = \frac{1}{N_1} + \left(\frac{1}{N_2^1 + N_2^2}\right) = \frac{N_1 + N_2^1 + N_2^2}{N_1 * (N_2^1 + N_2^2)} \quad (5)$$

whereN_2^1 and N_2^2 are the sums of states of the inner transition states for the addition of OH at C3 and C2, leading to the addition adducts P1 and P2, respectively.

The variational RRKM method [26] was used to minimize the sum of states along the reaction path. Ranges of energy up to 50 kcal mol^{-1} (ΔE = 0.5 kcal mol^{-1}) and *J* values from 0 to 200 (ΔJ=1) were considered in the calculation of the sum of states, in a total of 20100 values for each step.

Rate coefficients in the high-pressure limit, $k^{\infty}(T)$, were calculated as:

$$k^{\infty}(T) = \frac{1}{hQ_aQ_bQ_{rel}} \int_0^{\infty} \left[N_{eff}(E,J) x e^{-E/KT}\right] dJdE \quad (6)$$

Table 4
The microcanonical variational rate coefficient for OH-addition reactions,k_{add}(cm³ molec^{-1} s^{-1}),as a function of the temperature

Temperature (K)	k_{add} (cm³ molec^{-1} s^{-1})
200	3.45 x 10^{-12}
300	1.30 x 10^{-12}
400	8.52 x 10^{-13}
500	7.34 x 10^{-13}

Where Q_a and Q_b are partition functions for the reactants (electronic x vibrational x rotational) and Q_{rel} is the relative translational partition function.

Table 4 presents the resulting rate coefficients for addition reactions in the range of 200-500 K. It is important to highlight that for abstraction and addition mechanism for temperatures above 550 K the RRKM approach could not be done. As expected, the mCVTST rate coefficients are slightly lower than the CVTST rate coefficients, but since the difference between mCVTST and CVTST rate coefficients can be considered negligible, the mCVTST results validate the CVTST results.

Finally, we note that, from our best calculations, the global rate coefficient at 300 K, predicted as $k_{abs} + k_{add}$, is 1.37x10^{-12} cm^3 molec^{-1} s^{-1}, two order of magnitude lower than the experimental value [17]. Our predicted rate coefficients, as a function of the temperature, may also be underestimated by the same factor, due to small errors on the reaction energetics. This apparently high deviation, however, does not invalidate the theoretical model, but suggests that further corrections on the reaction energetics are still needed.

4. Conclusions

In this work, the potential energy surface for the reactions of OH with 2,5-dimethylfuran have been studied at a BHandHLYP/aug-cc-pVDZ and canonical and microcanonical variational rate coefficients also have been calculated. For the addition paths, our results indicate that the formation of a pre-reaction complex is determinant only for temperatures below 550 K. To the best of our knowledge, these results represents the first study that discriminates in details the effect of the formation of a pre-reaction complex in the reaction of OH radical with 2,5-dimethylfuran. This is an important contribution for the better comprehension of the reactions of DMF and other alkylfurans with hydroxyl radical, particularly about the addition mechanism. The global rate coefficients show that the addition of OH is an important decomposition path under atmospheric conditions at temperatures from 200 K to 300 K, but H abstraction by OH is practically negligible. The global rate coefficient at 300 K was predicted at $1.37 \cdot 10^{-12}$ $cm^3 \cdot molecule^{-1} \cdot s^{-1}$. Since it is a common understanding that OH radicals are the most important oxidant during the daytime, OH-addition may represent the principal degradation route for furan and its derivatives in the atmosphere at daylight. The results indicate k_{add} as a increasing function of the temperature above 550 K, suggesting that in combustions conditions this path may also be achieved. The H abstraction path becomes more important under combustion conditions. Our theoretical results may be of interest of combustion specialists, since DMF is a promising gasoline substitute, and atmospheric chemists, particularly those who work on aromatic molecules with conjugated double bonds.

5. Ackowledments

The authors thank CAPES and FAPERJ (E-26/010.003338/2014) for the financial support.

6. References

[1]B. Sirjean, R. Fournet, Phys. Chem. Chem. Phys. 15 (2013)596—611.

[2]J. M. Simmie, W. K. Metcalfe, J. Phys. Chem. A. 115 (2011) 8877–8888.

[3]K.P. Somers, J. M. Simmie, F. Gillespie, C. Conroy, G. Black, W.K. Metcalfe, F. Battin-Leclerc, P. Dirrenberger, O. Herbinet, P. A. Glaude, P. Dagaut, C. Togbé, K. Yasunaga, R. X. Fernandes, C. Lee, R.Tripathi, H. J. Curran, Combustion and Flame 160 (2013) 2291-2318.

[4]C. Togbé, L. Tran, D. Liu, D. Felsmann, P. Oßwald, P. Glaude, B. Sirjean, R. Fournet, F. Battin-Leclerc, K. Kohse-Höinghaus, Combustion and Flame 161 (2014) 780-797.

[5] Y. Román-Leshkov, C. J. Barrett, Z. Y. Liu, J. A. Dumesic, Nature 447(2007) 982-986.

[6] Y. Su, H. M. Brown, X. Huang, X. Zhou, J. E. Amonette, Z.C. Zhang, Appl. Catal., A 361 (1–2) (2009) 117–122.

[7] J.B. Binder, R.T. Raines, J. Am. Chem. Soc. 131 (5) (2009) 1979–1985.

[8] T. Thananatthanachon, T.B. Rauchfuss, Angew. Chem. 122 (37) (2010) 6766–6768.

[9] M. Chidambaram, A.T. Bell, Green Chem. 12 (7) (2010) 1253–1262.

[10]B. Sirjean, R. Fournet, P. Glaude, F. Battin-Leclerc, W. Wang, M. Oehlschlaeger, J. Phys. Chem. A117(2013) 1371-1392.

[11] A. Lifshitz, C. Tamburu, R. Shashua, J. Phys. Chem. A 102 (1998) 10655−10670.

[12] R. Atkinson, J. Arey, J. Chem. Rev. 103 (2003) 4605−4638.

[13] M. Francisco-Márquez, J. R. Alvarez-Idaboy, A. Galano, A. Vivier-Bunge, Environ. Sci. Technol. 39 (2005)8797-8802.

[14]B. Cabañas, F. Villanueva, P. Martín, M. T. Baeza, S. Salgado, E. Jiménez, Atmos. Environ. 39 (2005) 1935–1944.

[15] T. Luc-Sy, B. Sirjean, P. Glaude, K. Kohse-Höinghaus, F. Battin-Leclerc, Proc. Combust. Inst. 2014, http://dx.doi.org/10.1016/j.proci.2014.06.137.

[16] W. Zhang, B. Du, L. Mu,C.Feng, Int. J. Quantum Chem. 108 (2008) 1232−1238.

[17]A. Bierbach, I. Barnes, K. H. Becker, Atmos Environ.26 (1992) 813-817.

[18] I. N. Levine, Quantum Chemistry,Prentice Hall, Upper Saddle River N. J., 2000.

[19]A. D. Becke, J. Chem. Phys. 98 (1993) 1372-1377.

[20] T. H. Dunning JR., J. Chem. Phys. 1989 (1993)1007-1023.

[21] K. Fukui, J. Phys Chem. 74 (1970) 4161.

[22]M. J Frisch, G. W. Trucks, H. B. Schlegel, G. E. Scuseria, M. A. Robb, J. R Cheeseman, G. Scalmani, V. Barone, B. Mennucci, G. A. Petersson, H. Nakatsuji, M. Caricato, X. Li, H. P. Hratchian, A. F. Izmaylov, J. Blondo, G. Zheng, J. L. Sonnenberg, M. Hada, M. Ehara, K. Toyota, R. Fukuda, J. Hadsegawa, M. Ishida, T. Nakajima, Y. Honda, O. Kitao, H. Nakai, T. Vreven, J. A. Montgomery Jr, J. E. Peralta, F. Ogliaro, M. Bearpark, J. J. Heyd, E. Brothers, K. N. Kund, V. N. Staroverov, R. Kobayashi, J. Normand, K. Raghavachari, A. Rendell, J. C. Burant, S. S. Iyengar, J. Tomasi, M. Cossi, N. Rega, J. M. Millam, M. Klene, J. E. Knox, J. B. Cross, V. Bakken, C. Adamo, J. Jaramillo, R. Gomperts, R. E. Stratmann, O. Yazyev, A. J. Austin, R. Cammi, C. Pomelli, J. W. Ochterski, R. L. Martin, K. Morokuma, V. G. Zakrzewski, G. A. Voth, P. Salvador, J. J. Dannenberg, S. Dapprich, A. D. Daniels, ¨O. Farkas, J. B. Foresman, J. V. Ortiz, J. Cioslowski and D. J. Fox, Gaussian, Inc., Wallingford CT, Gaussian 03, Revision A.02, 2003.

[23] T. S. Barbosa, J. D. Nieto, P. M. Cometto, S. I. Lane, G. F. Bauerfeldt, G. Arbila, RSC Adv (4) (2014), 20830-20840.

[24]W. Zhang, B. Du, L. Mu, C. Feng, J. Mol. Struct. 851 (1-3) (2008) 353−357.

[25]J. M. Simmie, H. J. Curran, J. Phys. Chem. A. 113 (2009) 5128–5137.

[26] L. Zhu, W. L. Hase, Chem. Phys. Lett., 175 (1990) 117.